Check for updates

Original Research Article

Research on Mechanism of Microenvironment of Myeloma Being Restored by Allicin Regulating the Activity of Hedgehog Pathway Through miR-29b

Pharmacognosy Magazine
22(4) 1291–1300, 2026
© The Author(s) 2025
Article reuse guidelines:
in.sagepub.com/journals-permissions-india
DOI: 10.1177/09731296251388240
journals.sagepub.com/home/phm
Sage

Yanli Wang[1], Fen Xie[2], Ying Cai[1] and Ping Xiang[3]

Abstract

Background: The proliferation of myeloma cells could be affected partly by the interaction between microRNA-29b (miR-29b) and Hedgehog.
Objectives: The research on the mechanism of microenvironment of myeloma being restored by allicin, regulating the activity of Hedgehog pathway through miR-29b, was studied to develop theoretical evidence on the drug discovery for myeloma.
Materials and Methods: A model of mice with myeloma was established. They were divided into several groups, including a model group, a group with a low dose of allicin, a group with a medium dose of allicin, a group with a high dose of allicin, a Neurodazine group, a GDC-0449 group, and a group with a high dose of allicin and Neurodazine. The presentation of the related gene protein was detected, respectively.
Results: Presentation of the miR-29b gene was increased in groups with different doses of allicin. The presentation of miR-29b gene was increased notably in a group with a high dose of allicin and Neurodazine. Necrosis degree of tumor cells was improved partly through hematoxylin and eosin (H&E) coloration. The presentation of interferon gamma (IFN-γ) was increased, and the presentation of interleukin-17 (IL-17) was decreased. The activity of the Hedgehog pathway could be regulated by allicin through increasing the presentation of miR-29b. So, the microenvironment of myeloma could be improved.
Conclusion: Hedgehog could be activated by allicin through increasing the presentation of miR-29b. The growth of tumor cells could be restrained. The apoptosis of tumor cells could be promoted. So, the microenvironment of myeloma could be improved.

Keywords

Allicin, miR-29b, Hedgehog pathway, myeloma, microenvironment of myeloma

Received 12 March 2025; **revised** 24 July 2025; **accepted** 12 September 2025

Introduction

The development of myeloma could be affected by multiple factors, including the environment, chemical substances, and viruses. Osteolysis could be caused by the abnormal hyperplasia of phagocytes in the bone marrow. The microenvironment of the marrow could be affected, and the proliferation of tumor cells could be promoted. So, effective treatment was discussed in our study (Blade et al., 2022; Neumeister et al., 2022).

The allicin was extracted from garlic. It has multiple effects, such as diminishing inflammation, reducing antivirus, and reducing blood pressure. And the multi-kinds of bacilli, including *Bacillus typhi* and *Bacillus dysenteriae*, could be restrained by allicin effectively. The binding activity of deoxyribonucleic acid (DNA) could be reduced by allicin by restraining the activity of nuclear factor kappa B (NF-κB) (Barnabei et al., 2021). So, the growth of tumor cells could be restrained, and the microenvironment of lung cancer could

Yanli Wang and Fen Xie contributed equally to this work.
[1]Department of Orthopedics, Huanggang Central Hospital of Yangtze University, Huanggang, Hubei, China
[2]Department of Hand Surgery, Union Hospital, Tongji Medical College, Huazhong University of Science and Technology, Wuhan, Hubei, China
[3]Chongqing Preschool Education College, Chongqing, China

Corresponding author:
Ying Cai, Department of Orthopedics, Huanggang Central Hospital of Yangtze University, No. 16, Kaopeng Street, Huangzhou District, Huanggang, Hubei 438000, China.
E-mail: huaifuyi792@163.com

Creative Commons Non Commercial CC BY-NC: This article is distributed under the terms of the Creative Commons Attribution-NonCommercial 4.0 License (http://www.creativecommons.org/licenses/by-nc/4.0/) which permits non-Commercial use, reproduction and distribution of the work without further permission provided the original work is attributed as specified on the SAGE and Open Access pages (https://us.sagepub.com/en-us/nam/open-access-at-sage).

be improved. The synthesis of protein in tumor cells could be restrained. And the proliferation of tumor cells could be restrained partly through restraining the pathway of mechanistic target of rapamycin (mTOR) and insulin-like growth factor 1 receptor (IGF-1R) (Deleyto-Seldas and Efeyan, 2021; Ma et al., 2023). So, the microenvironment of carcinoma of the colon could be improved by allicin. The apoptosis could be prompted partly, and the release of inflammatory medium could be reduced by allicin through restraining the presentation of P38, extracellular signal-regulated kinase (ERK), and Src (Phan et al., 2023). So, tumor diseases could be prevented and treated by allicin. The development of myeloma regulated by allicin has still not been reported.

The apoptosis could be prompted, and the proliferation of myeloma cells could be affected by microRNA-29b (miR-29b), partly through increasing the presentation of Bax/Bcl-2 (Hassin & Oren, 2023). The presentation of Caspase-3, Caspase-12, and Cytc could be activated by allicin through regulating the presentation of miR-29b (Alam et al., 2022). So, the formation of an apoptotic body could be induced, and apoptosis could be prompted. The secretion of insulin-like growth factor 1 (IGF-1) and fibroblast growth factor (FGF) could be affected by allicin through regulating the presentation of miR-29b (Grassilli et al., 2022). So, the curative effect on tumor could be improved further. Whether the microenvironment of myeloma could be restored by allicin through regulating the presentation of miR-29b has not been reported.

The development of tumor could be affected by activating the Hedgehog pathway (Wang et al., 2022). And there was a certain connection with drug tolerance and the activity of the Hedgehog pathway. The migration of myeloma cells could be prompted by activating the Hedgehog pathway (Liu et al., 2022). The development of a tumor could be prompted. The activity of Hedgehog could be restrained by miR-29b through targeting the Smoothened and glioma-associated oncogene homolog 1 (Gli1) genes (Peng et al., 2022). So, the proliferation of tumor cells could be restrained further. The development of tumor could be affected by miR-29b through regulating the Hedgehog pathway (Luo et al., 2023). The activity of Hedgehog could be restrained by reducing the presentation of smoothened (SMO) and Gli1. So anti-tumor effect could be developed. So, the mechanism of the microenvironment of myeloma being restored by allicin, regulating the activity of the Hedgehog pathway through miR-29b, was discussed in our study to provide a certain theoretical basis for the treatment of myeloma.

Materials and Methods

Experimental Materials

Allicin (grade: RG, purity: 80%, Shaanxi Ciyuan Biotechnology Co., Ltd.). It was an organosulfur compound extracted from garlic. It had multiple kinds of effects, including antibiosis, inflammation, and reducing blood lipid. The liver could be protected, and gastrointestinal peristalsis could be increased. RPMI8226 cell plant (American Type Culture Collection (ATCC)); first antibody (brain-derived neurotrophic factor (BDNF), purity: 95%), batch number: FNab00859, Wuhan Optical Valley International Biology Co., Ltd.); secondary antibody (Epredia, purity: 98%, batch number: TA-999-DHBH, Beijing Murdick Biological Co., Ltd.); polymerase chain reaction (PCR) primer and reagent kit (Shanghai Caiyou Industrial Co., Ltd.); Hedgehog activator (Neurodazine, purity: 99%, batch number: HY-108439, MCE); Hedgehog inhibitor (GDC-0449, purity: 99.97%, batch number: HY-10440, MCE); ELISA (batch number: CB10001-Mu, Coibo Biotechnology Co., Ltd.); transmission electron microscopy (TEM) (HT-7800).

Animals: Forty-eight specific pathogen free (SPF)-grade male standard deviation (SD) mice, aged 6–8 weeks and weighing 18–22 g (Shanghai Kanglang Biotechnology Co., Ltd.).

Animals' Tests

Establishment of Model

All mice were raised in an environment with a temperature of (22 ± 2)°C and a relative humidity of (50 ± 10)%. Alternating light exposure was provided for 12 h of bright and 12 h of dark to ensure that all mice could freely eat and drink. The mice were intervened after 1 week of adaptive feeding. Six healthy mice were set as a healthy group. The other 42 mice were illuminated by a ray with 300 cGy (radioactive source: 60Co, dosage: 172 cGy) for 24 h. Then they were inoculated with thirty million RPMI18226 cells through the right neck back subcutaneously, with 1 mL of disposable medical syringes. The mouse model of myeloma was established. The mind, activity, and size of tumor volume in various groups were observed. After modeling, the mice were adaptively raised for 1 week. During this period, the mental state, food intake, and weight changes of the mice were observed daily, and abnormal individuals were excluded. The experimental plan was approved by the Animal Ethics Committee.

Animals' Intervention and Grouping

The healthy group received no intervention and was only used for baseline data control. Among the 42 rats in the model group, 18 were randomly selected for allicin intervention and evenly divided into: low-dose group (10 mg/kg), medium-dose group (20 mg/kg), and high-dose group (40 mg/kg). Another 12 were selected for Hedgehog expression intervention and evenly divided into: The Hedgehog activator group (Neurodazine, dose 5 mg/kg, dissolved in dimethyl sulfoxide (DMSO)) and the Hedgehog inhibitor group (GDC-0449, dose 10 mg/kg, dissolved in normal saline). The remaining 12 rats were randomly and equally divided into the combined intervention group (simultaneously given 40 mg/kg allicin and 5 mg/kg Neurodazine) and the model group

(intraperitoneally injected with the same volume of 0.9% NaCl). All the drugs were administered by intraperitoneal injection at a fixed time (8:00 AM) every day for 7 consecutive days. The body weight, tumor volume, and behavioral status of mice were recorded daily, and samples were collected for detection after the intervention ended.

Observational Indexes

Results of Model Establishment

The minds and activities of mice in every group were observed. Their weight, size of tumor volume, condition of tumor ulceration, and death cases were recorded every 2–3 days. The size of the tumor volume was determined by a vernier calliper. It was calculated with the formula RTV = $ab^2/2$ (cubic millimeter).

Detection of Blood Biochemical Indexes

The secretion condition of IFN-γ, TNF-α, and IL-17 was detected by enzyme-linked immunosorbent assay (ELISA).

Hematoxylin and Eosin (H&E) Dyeing

The tumor tissue was fixed with 15% formalin. Then they were dehydrated with gradient ethanol. They were embedded in paraffin. They were cut into sections with a thickness of 5 μm. The sections were numbered in order. They were dyed with H&E. Then, the thin film was observed. The magnification time was 400. The blood was taken from the orbital vein. They were detected with ELISA.

Detection in Cells

The samples were collected. They were washed with phosphate-buffered saline (PBS) three times every 10 min. They were placed for 1 h quietly. They were fixed with 1% of osmium acid for 1 h. They were washed with PBS three times every 10 min. They were dehydrated with ethanol. The ethoxyline resin, as Epon812, was embedded. They were soaked in an acetone mixture with a proportion of 1:1. They were embedded overnight. They were saturated with pure embedding medium. Then they were embedded for 48h. They were cut into sections with a microtome (Leica EM UC7). Then they were observed under HT-7800.

Detection the Relative Presentation Quantity of CD269 and CD317

Prepare the single-cell suspension and adjust the cell density to 5×10^5–1×10^6 cells/mL. The antigen of the cell membrane was detected with flow cytometry (FCM). The antibody was added to the samples. The homotypic reference tube was prepared. They were mixed evenly. They were placed for 20 min without light. They were detected with CellQuestPro software by FCM after hematolysis was performed randomly. The positive proportion and expression strength of CD269 and CD317 in cells were counted by adopting the joint gate combined with CD45/SSC and CD138. The positive cell was recorded when the positive rate of the membranous antigen was more than 20%.

PCR Detection

The homogenate was prepared after 1 mL of Trizol was added to the tumor tissue. Then they were mixed evenly after two hundred microliters of chloroform were added. They were centrifuged after the lamination was formed. The supernatant was collected and mixed with isopropanol. The ribonucleic acid (RNA) was precipitated after centrifugation. Then they were washed with absolute ethanol twice. Then they were dissolved in double-distilled water. The concentration of total RNA was detected. The RNA was transferred into complementary deoxyribonucleic acid (cDNA). The PCR primer and primer sequence are shown in Table 1.

Detection of WB Protein

The tissue was cut into pieces. Then they were added to the homogenizer. Then, radioimmunoprecipitation assay (RIPA) lysate was added to the centrifuge tube. The homogenate was prepared. They were centrifuged. The supernatant was collected. They were put into a centrifuge tube. Then they were preserved. The protein content was detected using the Bradford method. The electrophoresis and transmembrane were conducted. They were incubated after they were closed. The first antibody was added and incubated at 37°C and 5% CO_2 for 60 min, followed by the addition of the secondary antibody. The membrane was washed again. The enhanced chemiluminescence (ECL) was developed with a coloring instrument. The Bio-Rad ChemiDoc XRS and chemiluminescence imaging and analysis system were adopted. The

Table 1. Real-time Polymerase Chain Reaction (PCR) Prime and Prime Sequence.

Primer		Primer Sequence
miR-29b	Forward primer	5′-CTCCTGAGCGCAAGTACTCT-3′
	Reverse primer	5′-TACTCCTGCTTGCTGATCCAC-3′
GAPDH	Forward primer	5′-ATTACCCGCCCGACAATAGG-3′
	Reverse primer	5′-CATGAGTCAGCTAGGCTAGAA-3′

Note: GAPDH: Glyceraldehyde 3-phosphate dehydrogenase.

imaging pictures were analyzed with image analysis software as IPP6.0. The limit of detection (LOD) of pictures was analyzed.

Statistical Analysis

The data were analyzed using the Statistical Package for the Social Sciences (SPSS) 21.0 and GraphPad Prism. The results were represented as average values ± SD. The *F*-test was adopted. The difference among the data in every group was evaluated using the least significant difference (LSD) method. There was a notable difference when the *p* value was more than .05.

Results

Successful Establishment of Mice Model With Myeloma

Healthy group mice were irradiated with a single dose of 300 cGy X-rays (60Co source). After 24 h, 3×10^7 RPMI8226 cells were subcutaneously inoculated into the right dorsal cervical region. Subcutaneous nodules became palpable at the inoculation site by day 11 post-inoculation, exhibiting a skin-colored appearance. Tumor burden progressively increased between weeks 2 and 3 post-inoculation, with new nodules continuing to emerge through weeks 3–4. The tumor take rate reached 70%. Following initial detection, tumor volume showed time-dependent enlargement, peaking at weeks 5–6 post-inoculation. These findings confirmed the successful establishment of the myeloma mouse model (Figure 1).

The microenvironment of myeloma could be restored by allicin. There was an abnormal in Hedgehog pathway. The interferon gamma (IFN-γ) expression was gradually increased along with the increase in the allicin dosage. It was the highest in the group with high allicin dosage. The expression of TNF-α and IL-17 was notably declined along with the increase in allicin dosage (Figure 2A–2C). The miR-29b presentation was notably increased along with the increase in the allicin dosage when expression of the gene and protein of miR-29b and Hedgehog was detected. The microenvironment of mice with myeloma could be improved by allicin. It was related to the Hedgehog pathway (Figure 2D and 2E).



Figure 1. The Mice Model with Myeloma was Established Successfully.

Microenvironment of Myeloma Could Be Improved Through Activating the Activity of Hedgehog Pathway

There was a large number of plasmablasts and proplasmacytes in tumor group. The volume of tumor cells was large. There was a violet and a large cell nucleus. The chromatin was condensed under the nuclear envelope. There was a marked and massive. There were obvious classical Mitotic cells. There was a broken appearance and apoptosis in the GDC-0449 group. There was a loose appearance in the array at different degrees. There was a large number of cell necroses. There were broken cells in the Neurodazine group. The quantity of plasmablasts and proplasmacytes declined. There was obvious loose chromatin (Figure 3A). There was an abnormal-proliferated phagocyte in the autophagocyte. And the form was irregular. There was an invaginated state in the nuclear envelope. There were large vacuoles inside the cell nucleus (Figure 3B). The secreted condition of IFN-γ could be increased by injecting the activator and inhibitor in the Neurodazine group. The expression of TNF-α and IL-17 could be restrained. The gene expression of miR-29b could be increased. The effect was not notable in the GDC-0449 group. There was no notable difference between the GDC-0449 group and the model group (Figure 3C–3F).

Microenvironment of Myeloma Could Be Restored by Allicin Through the Activity of Hedgehog Pathway Being Activated by miR-29b

There was necrosis in tumor tissue and an obvious liquefied phenomenon in a group with high dosage allicin and Neurodazine (Figure 4A). The proportion of positive expression of CD269 and CD317 in the group with high dosage

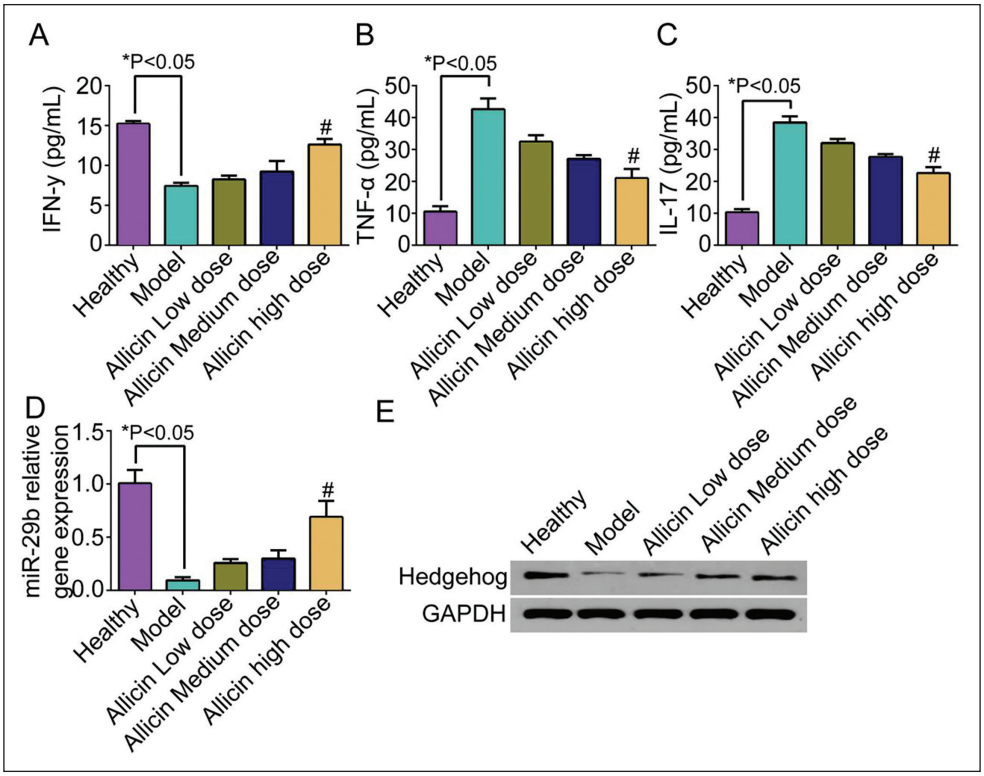


Figure 2. Condition of Expression of Gene and Protein in Every Group. (A) IFN-y Expression Detected with ELISA Method. (B) TNF-α Expression Detected with ELISA Method. (C) IL-17 Expression Detected with ELISA Method. (D) miR-29b Expression Detected with PCR Method. (E) Hedgehog Expression Detected with Western Blot Method. The * Represented Than $p < .05$ Compared with the Healthy Group. The # Represented That $p < .05$ Compared with the Model Group.Note: ELISA: Enzyme-linked immunosorbent assay; IFN-γ: Interferon gamma; IL-17: Interleukin-17; miR-29b: MicroRNA-29b; PCR: Polymerase chain reaction.

allicin and Neurodazine could be decreased effectively (Figure 4B and 4C). The expression of miR-29b group with high dosage allicin and Neurodazine was the highest compared with other groups. There was high expression (Figure 4D–4E).

Discussion

There were multiple myeloma (MM) cases in 10% of multiple kinds of hematological malignancies. It was caused by abnormal proliferation in phagocytes related to age and excessive generation of immunoglobulin (Ig) and M protein (Cai et al., 2023). The mean age of patients was 50–65. The frequency of MM was secretive. There were middle and late patients in the major group when they were diagnosed. There was also a transformation in Brugada syndrome (BrS). The M protein or Bence Jones protein (BJP) could often be detected in patients' blood or urine. However, the condition and therapeutic reaction of patients with oligocrine type could not be evaluated accurately through the detection of M protein. The allicin is an organosulfur compound separated from garlic bulbs. The multiple kinds of etiologic agents, including *Staphylococcus* and *Meningitis diococci*, could be restrained notably by allicin. The proliferation could be restrained. The cell cycle could be blocked. Immunization could be adjusted by allicin (Galgaye, 2023). The cells of gastric cancer could be partly restrained by allicin. The *in vitro* colony growth of the swing anti-blood cells could be restrained. The digestive tract cancer could be prevented by blocking the synthesis of nitrosamine (Charlinski & Jurczyszyn, 2022). The drug-resistance of stem cells in mammary cancer could be set back by allicin through restraining the abnormal activation of NF-kB and reducing the expression level of the downstream gene, a P-glycoprotein (P-gp). The tumor cells could be terminated directly by allicin. Tumor growth could be disturbed by regulating the body's immunologic function by allicin (Shi et al., 2019). The skin inflammation of psoriasis induced by Imiquimod could be improved by allincin through disturbing the interaction between Malpighian cells and interleukin-17A (IL-17A) (Zhou et al., 2022). The microenvironment of mice with myeloma could be improved by allicin from our study. It was related to the Hedgehog pathway. There was abnormal gene presentation of miR-29b in mice with myeloma through being co-intervened with allicin and Neurodazine. So, the microenvironment of mice with myeloma could be improved by allicin through the activity of Hedgehog being regulated by miR-29b.

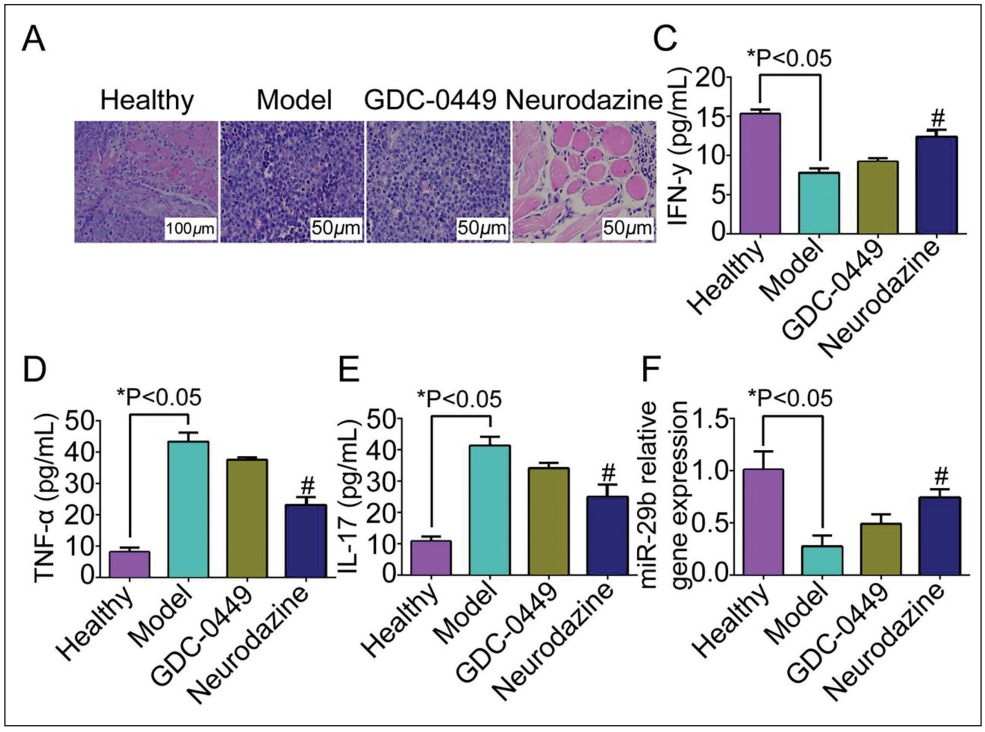


Figure 3. Microenvironment of Myeloma Could be Improved Through Activating the Activity of Hedgehog Pathway (n = 6). (A) Form of Cells in Every Group (Magnification was 400). (B) Performance of Autophagocyte in Tumor Cells (Magnification was 10,000). (C) Expression of IFN-γ was Detected with ELISA Method. (D) Expression of TNF-α was Detected with ELISA Method. (E) Expression of IL-17 was Detected with ELISA Method. (F) Expression of miR-29b was Detected with PCR Method. The * Represented Than $p < .05$ Compared with the Healthy Group. The # Represented That $p < .05$ Compared with the Model Group.Note: ELISA: Enzyme-linked immunosorbent assay; IFN-γ: Interferon gamma; IL-17: Interleukin-17; miR-29b: MicroRNA-29b; PCR: Polymerase chain reaction; TNF-α: Tumor necrosis factor alpha.

The presentation level of IFN-γ was gradually increased along with the increasing dosage of allicin from our study. The secreted condition of TNF-α and IL-17 could be notably declined. And the Hedgehog pathway was activated. The effect on improving the microenvironment of mice with myeloma could be better with the increasing dosage of allicin. It was related to the Hedgehog pathway. The multiple kinds of pharmacological effects of allicin, including anti-inflammation, reducing blood pressure, and anti-tumor, have been verified. The allicin has been found to develop the anti-cancer effect in multiple kinds of solid malignant tumor through strengthening the anti-tumor effect of macrophages, improving the immunologic function in patients with tumor, restraining the malignant biological behavior of cancer cells (Sarvizadeh et al., 2021). The cellular function could be regulated by TNF-α partly through inducing the interaction between tumor necrosis factor receptor 1 (TNF-R1) and tumor necrosis factor receptor 2 (TNF-R2). The apoptosis could be mainly induced by TNFR1. The Hedgehog pathway could be activated by TNF-R2 mainly through gathering the factors related to the TNF receptor to enter the cell nucleus. The specific binding site of the target gene could be combined with TNF-R2. So, apoptosis could be blocked through regulating the transcription of the target gene (Zhang et al., 2023). The Hedgehog pathway starts at three secreting types, concluding Sonic Hedgehog (SHh), Indian Hedgehog (IHh), and Desert Hedgehog (DHh). It could be combined with patched 1 (PTCH1). The IHh and SHh ligand in bone marrow was generated by bone marrow stromal cells (BMSC) (Che et al., 2023). There was apoptosis in 24 h of *in vitro* cultivated of MM cells if the cells were terminated. The proliferation of MM cells could be effectively prompted by multiple kinds of growth factors, including interleukin-3 (IL-3), interleukin-11 (IL-11), granulocyte-macrophage colony-stimulating factor (GM-CSF), stem cell factor (SCF), and Wnt family member 3A (Wnt3a), only when IHh or SHh was added to the culture medium. The survival proportion could be increased. There was an activated Hedgehog pathway in multiple kinds of tumor. So, the activation of the pathway was probably the key procedure of the malignant transformation of stem cells into tumor. The proliferation, migration, and invasion of tumor could be prompted (Li et al., 2023).

The Hedgehog pathway starts at three secreting types, concluding Sonic (SHh), Indian (IHh), and Desert (DHh). It could be combined with Patched (PTCH1) (Ingham, 2022). The IHh and SHh ligand in bone marrow was generated by

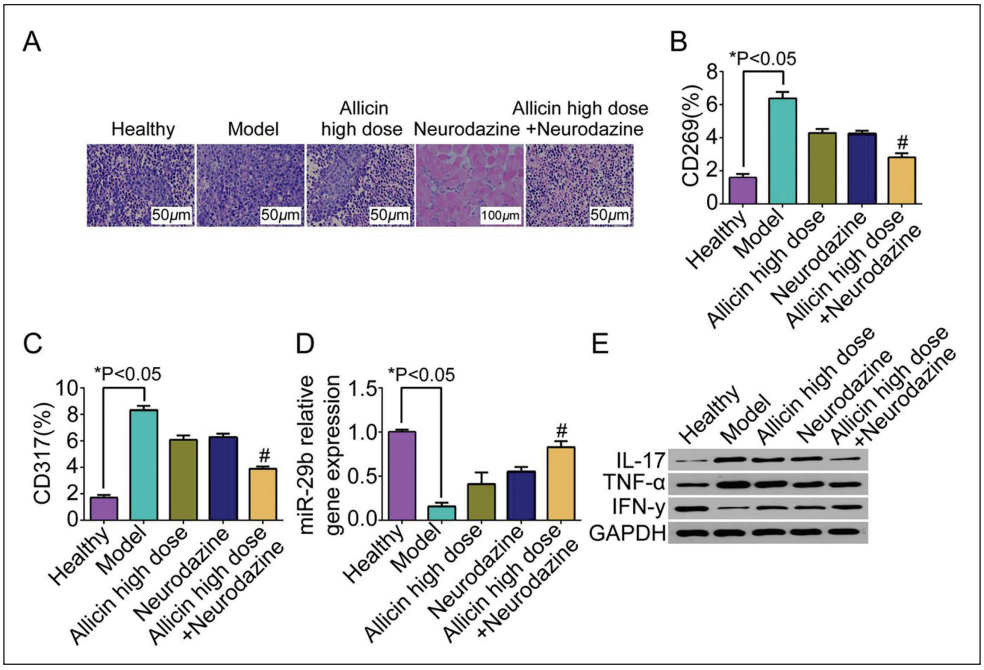


Figure 4. Microenvironment of Myeloma Could be Restored by Allicin Through the Activity of Hedgehog Pathway Being Activated by miR-29b (n = 6). (A) Form of Cells in Every Group (Magnification was 400). (B) Proportion of Positive Expression of CD269 in Marrow Cells. (C) Proportion of Positive Expression of CD317 in Marrow Cells. (D) Expression of miR-29b was Detected with PCR Method. (E) Result of Detection with Western Blot Method. The * Represented Than $p < .05$ Compared with the Healthy Group. The # Represented That $p < .05$ Compared with the Model Group.Note: miR-29b: MicroRNA-29b; PCR: Polymerase chain reaction.

BMSC (Giammona et al., 2023). There was apoptosis in 24 h of *in vitro* cultivated of MM cells if the cells were terminated. The proliferation of MM cells could be effectively prompted by multiple kinds of growth factors, including IL-3, IL-11, GM-CSF, SCF, and Wnt3a, only when IHh or SHh was added to the culture medium. The survival proportion could be increased. The presentation of SMO in CD138 in bone marrow cells could be increased if there was excessive presentation of multiple key regulatory factors. There was clone proliferation in these cells. The proliferation of cyclopamine could be restrained. It could also be induced to differentiate into mature $CD138^{+}$ cells. The Hedgehog pathway could develop biological effects mainly through regulating the expression of target genes. Cell growth and differentiation could be prompted. It could develop anti-cancer effects on multiple kinds of malignancy through regulating non-coding RNA, including long-chain and non-coding RNA, cyclic RNA, and microRNA. The peripheral neural remodeling (PNR) could be prompted by Hedgehog-Gli1 through the Hedgehog-Gli1 axis, and the Hedgehog signal could be activated. So, restoring the peripheral nervous system in pancreatic cancer could be induced. The presentation of actin could be affected directly by miRNA. Or multiple kinds of cascade reactions of cytoskeleton arrangement could be affected indirectly. The skeleton of actin could be restored partly. So, the transformation of mechanical factors in tumor microenvironment could be affected. The growth of tumor cells could be prompted by miRNA in patients through the above-mentioned mechanism in myeloma. The remodeling of the cellular framework could be induced partly. There is miRNA in the exosomes of patients with myeloma. The interleukin-6 (IL-6) and Ang-2 could be secreted. The presentation level of messenger ribonucleic acid (mRNA) could be changed. Hence, the microenvironment of tumor cells could be affected. The growth of marrow cells could be prompted (Katsushima et al., 2023). The apoptosis of tumor cells could be prompted by miR-29b. The DNA methylation of tumor could be restrained. The tumor proliferation could be reduced partly. The sensibility of chemotherapy could be increased. Thus, the body's immunologic function could be improved further. The growth of myocardial blood vessels and remodeling of the heart ventricle in mice with myocardial infarction could be improved through increasing the presentation of miR-29b-3p. Cardiac fibrosis and collagen volume fraction (CVF) could be reduced. The density of capillary vessels and expression of vascular endothelial growth factor (VEGF) could be increased. And apoptosis of cardiac cells could be restrained (Dai et al., 2023). The fibrillation of the aortic tunica media could be induced by miR-29b through increasing the presentation of the target gene (Pula et al., 2021). The remodeling and sclerosis of the aorta in diabetes mellitus could be regulated.

The presentation of miR-29b could be increased to different degrees in mice with myeloma after being injected with allicin at different dosages in our study. The gene presentation of miR-29b could be notably increased in groups with allicin at high dosage and Neurodazine. The degree of necrosis cells in tumor tissue could be improved from the H&E dyeing test. The presentation of IFN-γ was increased. The protein presentation of IFN-γ and IL-17 was decreased. The positive proportion of CD269 and CD317 gradually declined in the group with allicin at high dosage and Neurodazine. The microenvironment of myeloma could be restored by allicin through the activity of the Hedgehog pathway, which is regulated by miR-29b. The abnormal activity of Hedgehog pathway could play a crucial role in the occurrence and development of myeloma, the interaction between the microenvironment of bone marrow and marrow cells, and the features of stem cells in myeloma. The generation of osteoclasts could be reduced by Ishazomib (Zheng et al., 2022). Remodeling of bone could be regulated through activation of the classical Hedgehog pathway and promotion of the differentiation of osteoblasts. The complicated pathological condition of MM patients could be improved further. There was probably a relationship between the Hedgehog pathway and other signal pathways, such as Sirtuin 1 (SIRT1) and phosphoinositide 3-kinase/protein kinase B (PI3K/AKT) pathway. The occurrence and development of myeloma and self-maintaining of stem cells in myeloma could be co-affected. SIRT1 was induced by proteasome inhibitors. So, glioma-associated oncogene homolog 2 (GLI2) could be deacetylated. The synergistic reaction of SIRT1 and Hedgehog was found through enhancing the activity of the Hedgehog pathway in myeloma. It was the crucial mechanism for treating myeloma and improving drug resistance in myeloma (Schellinger et al., 2021).

Conclusion

In conclusion, Hedgehog pathway could be activated by allicin through regulating miR-29b. The activated Hedgehog pathway could exert its effect by regulating non-coding RNA and a downstream series of effectors. So, the microenvironment of myeloma could be remodeled. The presentation of tumor factors could be reduced. The apoptosis in tumor tissue could be improved. Certain theoretical evidence could be provided for the microenvironment of myeloma being restored by allicin in our study. But whether allicin could develop an effect through other signal pathways being regulated by miR-29b was still unclear. It still needs to be studied.

Abbreviations

ATCC: American Type Culture Collection; Bax: BCL2 associated X; Bcl-2: B-cell lymphoma 2; BDNF: Brain-derived neurotrophic factor; BJP: Bence Jones protein; BMSC: Bone marrow stromal cells; BrS: Brugada syndrome; cDNA: Complementary deoxyribonucleic acid; CVF: Collagen volume fraction; DHh: Desert Hedgehog; DMSO: Dimethyl sulfoxide; DNA: Deoxyribonucleic acid; ECL: Enhanced chemiluminescence; ELISA: Enzyme-linked immunosorbent assay; ERK: Extracellular signal-regulated kinase; FCM: Flow cytometry; FGF: Fibroblast growth factor; GAPDH: Glyceraldehyde 3-phosphate dehydrogenase; GDC-0449: Hedgehog inhibitor; Gli1: Glioma-associated oncogene homolog 1; Gli2: Glioma-associated oncogene homolog 2; GM-CSF: Granulocyte-macrophage colony-stimulating factor; H&E: Hematoxylin and eosin; HRP: Horseradish peroxidase; IFN-γ: Interferon gamma; Ig: Immunoglobulin; IGF-1: Insulin-like growth factor 1; IGF-1R: Insulin-like growth factor 1 receptor; IHh: Indian Hedgehog; IL-3: Interleukin-3; IL-6: Interleukin-6; IL-11: Interleukin-11; IL-17: Interleukin-17; IL-17A: Interleukin-17A; LOD: Limit of detection; LSD: Least significant difference; miR-29b: MicroRNA-29b; MM: Multiple myeloma; mRNA: Messenger ribonucleic acid; mTOR: Mechanistic target of rapamycin; NF-κB: Nuclear factor kappa B; P-gp: P-glycoprotein; P38: p38 mitogen-activated protein kinase; PBS: Phosphate-buffered saline; PCR: Polymerase chain reaction; PI3K/AKT: Phosphoinositide 3-kinase/protein kinase B; PNR: Peripheral neural remodeling; PTCH1: Patched 1; RIPA: Radioimmunoprecipitation assay; RNA: Ribonucleic acid; RTV: Relative tumor volume; SCF: Stem cell factor; SD: Standard deviation; SHh: Sonic Hedgehog; SIRT1: Sirtuin 1; SMO: Smoothened; SPF: Specific pathogen free; SPSS: Statistical package for the social sciences; TEM: Transmission electron microscopy; TNF-α: Tumor necrosis factor alpha; TNF-R1: Tumor necrosis factor receptor 1; TNF-R2: Tumor necrosis factor receptor 2; VEGF: Vascular endothelial growth factor; WB: Western blot; Wnt3a: Wnt family member 3A.

Acknowledgments

The authors gratefully acknowledge the Huanggang Central Hospital of Yangtze University for providing the necessary equipment for this study.

Declaration of Conflicting Interests

The author declared no potential conflicts of interest with respect to the research, authorship, and/or publication of this article.

Ethical Approval and Informed Consent

This study was approved by the Ethics Committee of Huanggang Central Hospital of Yangtze University.

Funding

The authors received no financial support for the research, authorship, and/or publication of this article.

ORCID iD

Ying Cai https://orcid.org/0009-0000-1952-6262

References

Alam, M., Alam, S., Shamsi, A., Adnan, M., Elasbali, A. M., Abu Al-Soud, W., Alreshidi, M., Hawsawi, Y. M., Tippana, A., Pasupuleti, V. R., & Hassan, M. I. (2022). Bax/Bcl-2 cascade is regulated by the EGFR pathway: Therapeutic targeting of

non-small cell lung cancer. *Frontiers in Oncology*, *12*, 869672. https://doi.org/10.3389/fonc.2022.869672

Barnabei, L., Laplantine, E., Mbongo, W., Rieux-Laucat, F., & Weil, R. (2021). NF-kappaB: At the borders of autoimmunity and inflammation. *Frontiers in Immunology*, *12*, 716469. https://doi.org/10.3389/fimmu.2021.716469

Blade, J., Beksac, M., Caers, J., Jurczyszyn, A., von Lilienfeld-Toal, M., Moreau, P., Rasche, L., Rosinol, L., Usmani, S. Z., Zamagni, E., & Richardson, P. (2022). Extramedullary disease in multiple myeloma: A systematic literature review. *Blood Cancer Journal*, *12*(3), 45. https://doi.org/10.1038/s41408-022-00643-3

Cai, E., Barba, M. G., & Ge, X. (2023). Hedgehog signaling in cortical development. *Cells*, *13*(1), 21. https://doi.org/10.3390/cells13010021

Charlinski, G., & Jurczyszyn, A. (2022). Non-secretory multiple myeloma: Diagnosis and management. *Advances in Clinical and Experimental Medicine*, *31*(1), 95–100. https://doi.org/10.17219/acem/141455

Che, H. Y., Zhou, C. H., Lyu, C. C., Meng, Y., He, Y. T., Wang, H. Q., Wu, H. Y., Zhang, J. B., & Yuan, B. (2023). Allicin alleviated LPS-induced mastitis via the TLR4/NF-κB signaling pathway in bovine mammary epithelial cells. *International Journal of Molecular Sciences*, *24*(4), 3805. https://doi.org/10.3390/ijms24043805

Dai, W. Q., Wu, X. L., Li, J. J., Tang, W. X., Wang, Y., Xu, W. Q., Han, D. Y., Xu, X. R., & Xu, X. F. (2023). Hedgehog-Gli1-derived exosomal circ-0011536 mediates peripheral neural remodeling in pancreatic cancer by modulating the miR-451a/VGF axis. *Journal of Experimental and Clinical Cancer Research*, *42*(1), 83. https://doi.org/10.1186/s13046-023-02894-9

Deleyto-Seldas, N., & Efeyan, A. (2021). The mTOR-autophagy axis and the control of metabolism. *Frontiers in Cell and Developmental Biology*, *9*, 655731. https://doi.org/10.3389/fcell.2021.655731

Galgaye, G. G. (2023). Phenology, growth, yield, and yield-related traits of Ethiopian garlic genotypes. A review. *Heliyon*, *9*(6), e16497. https://doi.org/10.1016/j.heliyon.2023.e16497

Giammona, A., Crivaro, E., & Stecca, B. (2023). Emerging roles of hedgehog signaling in cancer immunity. *International Journal of Molecular Sciences*, *24*(2), 1321. https://doi.org/10.3390/ijms24021321

Grassilli, S., Bertagnolo, V., & Brugnoli, F. (2022). Mir-29b in breast cancer: A promising target for therapeutic approaches. *Diagnostics*, *12*(9), 2139. https://doi.org/10.3390/diagnostics12092139

Hassin, O., & Oren, M. (2023). Drugging p53 in cancer: One protein, many targets. *Nature Reviews Drug Discovery*, *22*(2), 127–144. https://doi.org/10.1038/s41573-022-00571-8

Ingham, P. W. (2022). Hedgehog signaling. *Current Topics in Developmental Biology*, *149*, 1–58. https://doi.org/10.1016/bs.ctdb.2022.04.003

Katsushima, K., Pokhrel, R., Mahmud, I., Yuan, M. L., Murad, R., Baral, P., Zhou, R., Chapagain, P., Garrett, T., Stapleton, S., Jallo, G., Bettegowda, C., Raabe, E., Wechsler-Reya, R. J., Eberhart, C. G., & Perera, R. J. (2023). The oncogenic circular RNA is a potential therapeutic target in sonic hedgehog-subtype childhood medulloblastomas. *Acta Neuropathologica Communications*, *11*(1), 145. https://doi.org/10.1186/s40478-023-01521-0

Li, P. T., Huang, Y., Wang, J., Zeng, J. S., & Li, L. (2023). Platycodin D relieves rheumatoid arthritis by promoting apoptosis of mitochondria to inhibit activation of hedgehog pathway. *Autoimmunity*, *56*(1), 12. https://doi.org/10.1080/08916934.2023.2205053

Liu, J. Q., Xiao, Q., Xiao, J. N., Niu, C. X., Li, Y. Y., Zhang, X. J., Zhou, Z. W., Shu, G., & Yin, G. (2022). Wnt/β-catenin signalling: function, biological mechanisms, and therapeutic opportunities. *Signal Transduction and Targeted Therapy*, *7*(1), 1–42. https://doi.org/10.1038/s41392-021-00762-6

Luo, J. J., Lu, C. J., Chen, Y., Wu, X. W., Zhu, C. C., Cui, W., Yu, S. C., Li, N. N., Pan, Y. H., Zhao, W. J., Yang, Q. K., & Yang, X. J. (2023). Nuclear translocation of cGAS orchestrates VEGF-A-mediated angiogenesis. *Cell Reports*, *42*(4), 112328. https://doi.org/10.1016/j.celrep.2023.112328

Ma, L., Zhao, W., Huang, S., Xu, F., Wang, Y., Deng, D., Zhang, T., Shu, S., & Chen, X. (2023). IGF/IGF-1R signal pathway in pain: a promising therapeutic target. *International Journal of Biological Sciences*, *19*(11), 3472–3482. https://doi.org/10.7150/ijbs.84353

Neumeister, P., Schulz, E., Pansy, K., Szmyra, M., & Deutsch, A.J. (2022). Targeting the microenvironment for treating multiple myeloma. *International Journal of Molecular Sciences*, *23*(14), 7627. https://doi.org/10.3390/ijms23147627

Peng, D. D., Fu, M. Y., Wang, M. N., Wei, Y. Q., & Wei, X. W. (2022). Targeting TGF-β signal transduction for fibrosis and cancer therapy. *Molecular Cancer*, *21*(1), 104. https://doi.org/10.1038/s41392-020-00436-9

Phan, T., Zhang, X.H., Rosen, S., & Melstrom, L.G. (2023). P38 kinase in gastrointestinal cancers. *Cancer Gene Therapy*, *30*(9), 1181–1189. https://doi.org/10.1038/s41417-023-00622-1

Pula, A., Robak, P., Mikulski, D., & Robak, T. (2021). The significance of mRNA in the biology of multiple myeloma and its clinical implications. *International Journal of Molecular Sciences*, *22*(21), 12070. https://doi.org/10.3390/ijms222112070

Sarvizadeh, M., Hasanpour, O., Ghale-Noie, Z. N., Mollazadeh, S., Rezaei, M., Pourghadamyari, H., Khooy, M. M., Aschner, M., Khan, H., Rezaei, N., Shojaie, L., & Mirzaei, H. (2021). Allicin and digestive system cancers: From chemical structure to its therapeutic opportunities. *Frontiers in Oncology*, *11*, 650256. https://doi.org/10.3389/fonc.2021.650256

Schellinger, I. N., Wagenhäuser, M., Chodisetti, G., Mattern, K., Dannert, A., Petzold, A., Jakubizka-Smorag, J., Emrich, F., Haunschild, J., Schuster, A., Schwob, E., Schulz, K., Maegdefessel, L., Spin, J. M., Stumvoll, M., Hasenfuss, G., Tsao, P. S., & Raaz, U. (2021). MicroRNA miR-29b regulates diabetic aortic remodeling and stiffening. *Molecular Therapy-Nucleic Acids*, *24*, 188–199. https://doi.org/10.1016/j.omtn.2021.02.021

Shi, X. E., Zhou, X. M., Chu, X. Y., Wang, J., Xie, B. C., Ge, J., Guo, Y., Li, X., & Yang, G. S. (2019). Allicin improves metabolism in high-fat diet-induced obese mice by modulating the gut microbiota. *Nutrients*, *11*(12), 2909. https://doi.org/10.3390/nu11122909

Wang, J., Hu, K., Cai, X., Yang, B., He, Q., Wang, J., & Weng, Q. (2022). Targeting PI3K/AKT signaling for treatment of idiopathic pulmonary fibrosis. *Acta Pharmaceutica Sinica B*, *12*(1), 18–32. https://doi.org/10.1016/j.apsb.2021.07.023

Zhang, L., Ma, X. H., Shi, R. M., Zhang, L. B., Zhao, R. L., Duan, R., Qin, Y. Y., Gao, S. J., Li, X. X., Duan, J. J., & Li, J. G. (2023). Allicin ameliorates imiquimod-induced psoriasis-like

skin inflammation via disturbing the interaction of keratinocytes with IL-17A. *British Journal of Pharmacology*, *180*(5), 628–646. https://doi.org/10.1111/bph.15983

Zheng, J. L., Zhang, X. J., Cai, W. F., Yang, Y. W., Guo, T., Li, J. M., & Dai, H. L. (2022). Bone marrow mesenchymal stem cell-derived exosomal microRNA-29b-3p promotes angiogenesis and ventricular remodeling in rats with myocardial infarction by targeting ADAMTS16. *Cardiovascular Toxicology*, *22*(8), 689–700. https://doi.org/10.1007/s12012-022-09745-7

Zhou, Y., Li, X. X., Luo, W. Y., Zhu, J. F., Zhao, J. W., Wang, M. Y., Sang, L. X., Chang, B., & Wang, B. Y. (2022). Allicin in digestive system cancer: From biological effects to clinical treatment. *Frontiers in Pharmacology*, *13*, 903259. https://doi.org/10.3389/fphar.2022.903259